Procrustes Analysis for Diffusion Tensor Image Processing

Diwei Zhou, Ian L. Dryden, Alexey A. Koloydenko, and Li Bai

***Abstract*—There is an increasing need to develop processing tools for diffusion tensor image data with the consideration of the non-Euclidean nature of the tensor space. In this paper Procrustes analysis, a non-Euclidean shape analysis tool under similarity transformations (rotation, scaling and translation), is proposed to redefine sample statistics of diffusion tensors. A new anisotropy measure Procrustes Anisotropy (PA) is defined with the full ordinary Procrustes analysis. Comparisons are made with other anisotropy measures including Fractional Anisotropy and Geodesic Anisotropy. The partial generalized Procrustes analysis is extended to a weighted generalized Procrustes framework for averaging sample tensors with different fractions of contributions to the mean tensor. Applications of Procrustes methods to diffusion tensor interpolation and smoothing are compared with Euclidean, Log-Euclidean and Riemannian methods.**

***Index Terms*—Non-euclidean metric, diffusion tensor, procrustes analysis, anisotropic diffusion.**

I. Introduction

Diffusion tensor imaging (DTI) is a specific magnetic resonance imaging (MRI) modality method for providing information about the microstructure and organization of the tissue in vivo. In DTI, displacement of water molecules over time is modeled by a zero-mean trivariate Gaussian distribution [1] with covariance matrix evolving linearly with time and determined by the diffusion tensor (DT), a 3x3 symmetric positive-definite matrix. DT inference from observed diffusion MRI data has been commonly carried out using least squares [2] [3] and Bayesian [4] [5] methods. The principal eigenvector of the tensor estimates the dominant fiber orientation at a voxel whereas various tensor-derived diffusion anisotropy indices measure local anisotropy. DTI has been applied into the study of diseases such as multiple sclerosis, schizophrenia, and stroke [6]. White matter tractography [7] [8] [9] is another promising application of DTI for investigating brain connectivity.

There is an increasing need to develop processing tools for diffusion tensor data. With the consideration of positive semi-definiteness and symmetry of diffusion tensor, non-Euclidean methods [10]-[14] have been proposed for diffusion tensor processing and anisotropy study.

Manuscript received June 25, 2012; revised August 18, 2012. The work was supported by the European Commission FP6 Marie Curie program through the CMIAG Research Training Network.

Diwei Zhou is with the School of Technology, University of Wolverhampton, Wolverhampton, WV1 1LY, UK (e-mail: d.zhou@wlv.ac.uk).

Ian L. Dryden is with the Department of Statistics, University of South Carolina, Columbia, SC 29208, USA.

Alexey A. Koloydenko is with the Department of Mathematics, Royal Holloway, University of London, Egham, TW20 0EX, UK.

Li Bai is with the School of Computer Science, University of Nottingham, Nottingham, NG8 1BB, UK

Recall that D is a 3x3 real matrix with symmetric positive semi-definiteness, i.e. $D = D^T$ and $xDx^T \geq 0$ for all real x. Let $f(D)$ be a probability density function of a diffusion tensor D on a Riemannian metric space. The Fréchet mean [14] [15] [16] of D is defined as

$$T = \arg \inf_T \frac{1}{2} \int d(D,T)^2 f(D) dD, \quad (1)$$

where d is a metric. A Fréchet mean is not necessarily unique. However, it is possible to prove the uniqueness with sufficient conditions. For example, for non-Euclidean spaces with negative sectional curvature, the Fréchet mean is always unique [17].

Given a sample of N diffusion tensors $D_1,\ldots,D_N$ the Fréchet mean of $D_1,\ldots,D_N$ is given by

$$\hat{T} = \arg \inf_T \sum_{i=1}^{N} d(D_i,T)^2. \quad (2)$$

And the sample variance of $D_1,\ldots,D_N$ is defined as

$$\sigma^2_{\mathbf{D}_1,\ldots,\mathbf{D}_N} = \frac{1}{N} \sum_{i=1}^{N} d(\mathbf{D}_i, \hat{\mathbf{T}})^2. \quad (3)$$

The Euclidean [18], Log-Euclidean [19] and Riemannian [14], [20] metrics, denoted by d_E, d_L and d_R respectively, have been proposed for defining the sample mean of diffusion tensors.

The main aim of this work is to define new statistics of diffusion tensor sample with the non-Euclidean method Procrustes analysis for tensor field processing and anisotropy study.

II. Procrustes Mean Diffusion Tensor

A. Procrustes Distances

In this section, two Procrustes-based distances full ordinary Procrustes and Procrustes size-and-shape distances will be introduced.

To ensure the positive semi-definiteness of D_i, $i = 1, 2$, we use a reparameterization $D_i = Q_i Q_i^T$ where Q_i is a 3x3 real matrix. For example, $Q_i = \text{chol}(D_i)$ is the Cholesky decomposition, or $Q_i = D_i^{1/2}$ is the matrix square root. In our computation we shall choose the Cholesky decomposition. Note that Q_i and any rotation of it Q_iR ($R \in O(3)$) result in the same D_i, i.e. $D_i = Q_i Q_i^T = Q_iR (Q_iR)^T$.

Full ordinary Procrustes analysis (FOPA) [21] [22] is used to match two objects as closely as possible with similarity transformations (translation, rotation and scale). Let us first consider a pair of diffusion tensors D_1 and D_2. The full Procrustes shape metric between D_1 and D_2 is given by

$$d_F(D_1,D_2) = \left\| Q_1 - \hat{\beta} Q_2 \hat{R} \right\| \quad (4)$$

where $(\hat{\beta}, \hat{R})$ is the solution to minimize a squared Euclidean distance under the similarity transformations. The squared Euclidean distance is given by

$$S_{FOPA}(D_1,D_2)^2 = \left\| Q_1 - \beta Q_2 R - 1_3 \gamma^T \right\|^2, \quad (5)$$

where a 3 x 3 rotation matrix $R \in O(3)$, a scale parameter $\beta > 0$, and a 3 x 1 location vector γ represent three similarity transformations. Note 1_3 is the 3 x 1 vector of ones. The solution $(\hat{R}, \hat{\beta}, \hat{R})$ to the minimization of (5) has been solved [21].

In DTI study, we wish to match Q_1 (from D_1) and Q_2 (from D_2) under location, rotation and reflection while often preserving scale information. Then the joint study of size-and-shape is of interest. Size-and-shape spaces were introduced by [23]. The definition of the size-and-shape of a configuration matrix was given by [21]. The Procrustes size-and-shape distance between two diffusion tensors is defined as

$$d_S(D_1,D_2) = \inf_{R \in o(3)} \left\| Q_1 - Q_2 R \right\| \quad (6)$$

The Procrustes solution $\hat{R}$ for matching Q_1 and Q_2 is

$$\hat{R} = \arg \inf_{R \in o(3)} \left\| Q_1 - Q_2 R \right\| = UV^T \quad (7)$$

where U and V are from the singular value decomposition.

B. Procrustes Estimators

Consider the general case where there are $N \geq 2$ diffusion tensors $D_1,\ldots,D_N$, and $D_i = Q_i Q_i^T$, $i = 1,2$. Now the aim is to calculate the Fréchet mean using the full Procrustes shape metric in (4) and the Procrustes size-and-shape metric in (6).

The sample Fréchet mean relative to the full Procrustes shape metric $d_F(\cdot)$ is given by

$$\hat{T}_F = \hat{Q}_F \hat{Q}_F^T, \quad (8)$$

where

$$\hat{Q}_F = \arg \inf_{Q} \sum_{i=1}^{N} \inf_{R \in o(3)} \left\| \beta_i Q_i R_i - Q \right\|^2. \quad (9)$$

The sample Fréchet mean relative to the Procrustes size-and-shape distance $d_S(\cdot)$ is given by

$$\hat{T}_F = \arg \inf_{T} \sum_{i=1}^{N} d_S(D_i,T)^2. \quad (10)$$

Specifically,

$$\hat{T}_S = \hat{Q}_S \hat{Q}_S^T, \quad (11)$$

where

$$\hat{Q}_S = \arg \inf_{Q} \sum_{i=1}^{N} \inf_{R \in o(3)} \left\| Q_i R_i - Q \right\|^2. \quad (12)$$

C. Procrustes Anisotropy

We define a new anisotropy measure Procrustes anisotropy (PA) with the full Procrustes shape metric. The definition of PA is given by

$$PA(D) = \sqrt{\frac{3}{2}} d_F\left(\frac{I_{3x3}}{\sqrt{3}}, D\right) = \sqrt{\frac{3}{2} \sum_{i=1}^{3} \left(\sqrt{\lambda_i} - \overline{\sqrt{\lambda}}\right)^2 / \sum_{i=1}^{3} \lambda_i} \quad (13)$$

where $\overline{\sqrt{\lambda}} = \sum_{i=1}^{3} \sqrt{\lambda_i} / 3$. It is clear that PA is a normalization of the FOPA distance from any given diffusion tensor D to the identity tensor, representing the case of ideal isotropy. The range of PA is [0, 1] with PA=0 indicating full isotropy and PA ≈ 1 representing the extremely strong anisotropy. PA is invariant to the uniform scaling of a diffusion tensor.

III. Weighted Generalized Procrustes Method

In this section, diffusion tensor processing methods including smoothing and interpolation are developed with consideration of contributions from more than two neighboring tensors.

A. Weighted Generalized Procrustes Analysis

For processing a sample of diffusion tensors at voxels distributed in three-dimensional space, a more general case appears that the contributions from $D_1,\ldots,D_N$ are different to the mean diffusion tensor. Therefore, we need to consider a weighted problem to obtain the weighted mean diffusion tensor.

Given a suitable distance function d, the weighted Fréchet sample mean of $D_1,\ldots,D_N$ is defined by:

$$T = \arg \inf_{D} \sum_{i=1}^{N} w_i d(D_i, D)^2, \quad (14)$$

where the weights w_i satisfy $w_i \geq 0$ and $\sum_{i=1}^{N} w_i = 1$, and in applications can be, for example, a function of the Euclidean distance from the location of interest to the sampling locations (e.g., voxels).

Weighted generalized Procrustes analysis (WGPA) is proposed to estimate $\hat{T}$ when $d = d_S$ is the size-and-shape distance [13]. It can then be shown that the WGPA mean tensor is given by

$$\hat{T}_{WGPA} = \hat{Q}_{WGPA} \hat{Q}_{WGPA}^T \quad (15)$$

where $\hat{Q}_{WGPA} = \sum_{i=1}^{N} w_i Q_i \hat{R}_i$ and the orthogonal matrices $\hat{R}_i$, $i=1,\ldots\ldots,N$ minimize S_{WGPA}, the sum of weighted squared Euclidean norms, which is given by

$$S_{WGPA} = \inf_{R_1,\ldots R_N} \sum_{i=1}^{N} w_i \left\| Q_i R_i - \sum_{j=1}^{N} w_j Q_j R_j \right\|^2. \quad (16)$$

B. Weights

In WGPA we assume that the weights w_i, i=1,....., N are a function of the Euclidean distance from the voxel of interest to the sampling voxel. The simplest setting for the weights is with the inverse distance function given by

$$w_i = \frac{d_i^{-1}}{\sum_{j=1}^{N} d_j^{-1}}, i = 1,\ldots\ldots,N \quad (17)$$

where d_i is the Euclidean distance from the voxel containing the weighted mean to the ith voxel with D_i.

For more flexibility of weight setting, an exponential

weight function is proposed as follows:

$$w_i = \frac{\exp(-Ad_i^2) + B}{\sum_{j=1}^{N} \exp(-Ad_j^2) + B}, i = 1,..., N \qquad (18)$$

where $A, B \geq 0$ are used to control the change of the weight as the distance changes. For example, with $A = 1$ and $B = 0.01$ the weight changes more steadily than the weight with $A = 20$ and $B = 0.01$.

Below we give an algorithm (in Table I) for computing $\hat{Q}_{WGPA}$

1: Initial setting: $\mathbf{Q}_i^P \leftarrow chol(\mathbf{D}_i), i = 1,..., N$

2: S_{WGPA} from previous iteration: $S_p \leftarrow 0$

3: S_{WGPA} from current iteration:

$S_p \leftarrow \sum_{i=1}^{N} w_i \| \mathbf{Q}_i^P - \sum_{j=1}^{N} w_j \mathbf{Q}_j^P \|^2$

4: while $| S_p - S_c |>$ tolerance do

5: for i=1 to N do

6: $\hat{\mathbf{Q}}_i = \frac{1}{1 - w_i} \sum_{j \neq i} w_i \mathbf{Q}_i^P$

7: Calculate the $\hat{\mathbf{R}}_i$ minimizing $\| \hat{\mathbf{Q}}_i - \mathbf{Q}_i^P \mathbf{R}_i \|$ (partial ordinary Procrustes analysis)

8: $\mathbf{Q}_i^P \leftarrow \mathbf{Q}_i^P \hat{\mathbf{R}}_i$

9: end for

10: $S_p \leftarrow S_c$

11: $S_c \leftarrow \sum_{i=1}^{N} w_i \| \mathbf{Q}_i^P - \sum_{j=1}^{N} w_j \mathbf{Q}_{ji}^P \|^2$

12: end while

13: $\hat{\mathbf{Q}}_{WGPA} \leftarrow \sum_{i=1}^{N} w_i \mathbf{Q}_i^P$

14: return $\hat{\mathbf{Q}}_{WGPA}$

C. Weights

In WGPA we assume that the weights wi, i=1,....., N are a function of the Euclidean distance from the voxel of interest to the sampling voxel. The simplest setting for the weights is with the inverse distance function given by

$$w_i = \frac{d_i^{-1}}{\sum_{j=1}^{N} d_j^{-1}}, i = 1,....., N \qquad (19)$$

where di is the Euclidean distance from the voxel containing the weighted mean to the *ith* voxel with D_i.

For more flexibility of weight setting, an exponential weight function is proposed as follows:

$$w_i = \frac{\exp(-Ad_i^2) + B}{\sum_{j=1}^{N} \exp(-Ad_j^2) + B}, i = 1,..., N \qquad (20)$$

where $A, B \geq 0$ are used to control the change of the weight as the distance changes. For example, with $A = 1$ and $B = 0.01$ the weight changes more steadily than the weight with $A = 20$ and $B = 0.01$.

D. Smoothing

Weighted generalized Procrustes framework can be adapted to smooth the diffusion tensor data. Let V_s be the voxel location in (x,y,z) coordinates. Let D_s be the original diffusion tensor in voxel V_s. Neighbor voxels of V_s can be defined by

$$\{V_1, V_2, \ldots, V_m\} = \arg_{V} ||V - V_s|| \leq d^* \qquad (21)$$

where $d^* \geq 0$ is a constant.

Given $D_1,\ldots,D_m$ at voxels $V_1,...,V_m$, the weighted mean $\overline{D}_s$ is the weighted generalized Procrustes mean of $D_1,\ldots,D_m$ and D_{m+1}, where $D_{m+1} = D_s$. It is natural to let D_s contribute to the weighted mean, and let V_s be a neighbor of itself, i.e. $V_s = V_{m+1}$. Weights of each diffusion tensor can be set with a weight function. For example, the exponential weights are given by

$$w_i = \frac{\exp(-A\|V_i - V_s\|^2) + B}{\sum_{j=1}^{N} [\exp(-A\|V_j - V_s\|^2) + B]}, \; i = 1,..., m+1. \qquad (21)$$

In particular, since $\|V_{m+1} - V_s\| = 0$, D_s with the largest weight w_{m+1} contributes most.

In a diffusion tensor dataset given each diffusion tensor D_s at voxel V_s and $D_1,\ldots,D_N$ at neighbour voxels $V_1,...,V_N$ we can calculate the weighted mean tensor $\overline{D}_s$ which will replace each D_s. The weights $w_1,...,w_N$ and w_s are set as proposed in (18).

E. Interpolation

By interpolation of the tensor data we mean construction of new diffusion tensors based on the original data. More specifically, we mesh the three-dimensional volume containing diffusion tensor data with regular rigid. For each new born subvoxel V^*, we will sample a weighted generalized Procrustes mean of diffusion tensors at V^*s neighbors, and allocate this mean to V^*.

IV. Applications

A. Material

A set of diffusion weighted MR images acquired with the Uniform 32 DTI diffusion gradient direction scheme [24] from a healthy human brain has been used for this study. The MR images were acquired using a spin echo EPI (echo planar imaging) sequence with diffusion weighting gradients applied with a weighting factor of b=1000 s/mm^2 in a Philips 3T Achieva clinical imaging system (Philips Medical Systems, Best, The Netherlands). Throughout the subject's head, 52 interleaved contiguous transaxial slices were acquired in a matrix of 112 x 112 (interpolated to 224 x 224) with an acquisition voxel size of 1x1x2 mm^3. For each slice, the acquisition was repeated for each of the 32 non-collinear directions according to the Uniform 32 direction scheme, and once with no diffusion weighting (b=0). A Bayesian estimation method [5] has been employed

to compute the tensor field and all methods of this paper are programmed with MATLAB (The Mathworks, Inc., R2008a).

B. Anisotropy Study

Now let us compare PA with Fractional Anisotropy (FA) [25], and the hyperbolic tangent function of Geodesic Anisotropy (tanh(GA)) [12] from real data. Fig. 1 shows FA, PA and tanh(GA) maps (axial slices). Since PA of diffusion tensor is always smaller than FA and tanh(GA) values, the PA map gives a darker color overall. The splenium in corpus callosum is one of the regions where the overall anisotropy is strongly high [26]. We take FA, PA and tanh(GA) values along the green line in the splenium and show them in Fig. 2. PA has significantly higher variation than FA and tanh(GA). In general, PA offers better contrast in highly anisotropic regions.

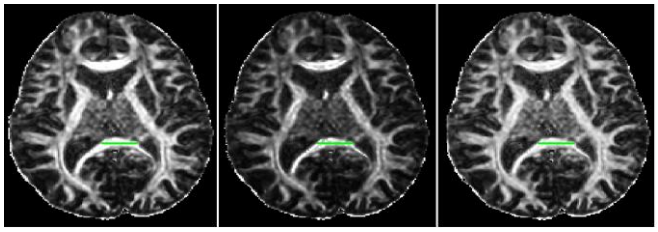

Fig. 1. Anisotropy maps from axial view. Left: FA map. Middle: PA map. Right: tanh(GA) map.

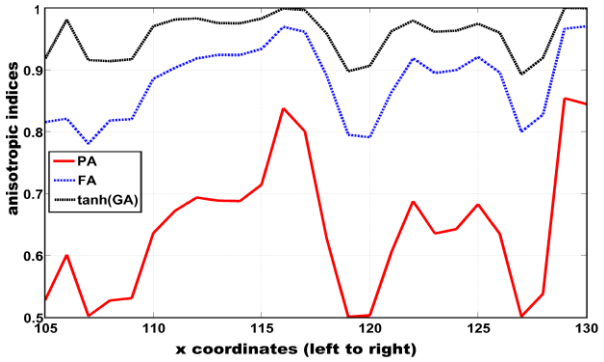

Fig. 2. Comparison of FA, PA and *tanh*(GA) values. FA, PA and *tanh*(GA) values are from tensors at voxels along the green line in Fig. 1.

C. Geodesic Interpolation

Now we carry out an experiment to investigate the geometric nature of geodesic paths obtained with different metrics.

Two synthetic tensors D_1 and D_2 are not orthogonal and are of different shape and size. To compare interpolations with different metrics in size, orientation and anisotropy of tensor, we use four measures: the determinant |D| (volume of the diffusion ellipsoid), |D|, FA and PA, where the angle ϕ measures the difference of orientations from the synthetic D_1 to an interpolated tensor in the geodesic path. The angle ϕ is the smaller angle between the principal eigenvectors of D_1 and the interpolated tensor. The angle ϕ is defined as

$$\phi = \arcsin(\| pv_1 \times pv_i \|),\ i = 1,.....,9 \qquad (22)$$

where pv_1 is the principal eigenvector of D_1 and pv_i is the principal eigenvector of the ith interpolated tensor (including two synthetic diffusion tensors), and i=1,…...,9, with i=1 and i=9 corresponding to the synthetic tensors D_1 and D_2, respectively.

Fig. 3. shows four different geodesic paths between D_1 and D_2, namely, the Euclidean d_E, log-Euclidean d_L, Riemannian d_R and Procrustes size-and-shape d_S metrics. From a variety of examples it does seem clear that the Euclidean metric is very problematic, especially due to the parabolic interpolation of the determinant. The Procrustes metric offers somewhat better interpolation in the tensor's orientation and anisotropy (see graphs of |D| and ϕ). In general, the log-Euclidean and Procrustes size-and-shape methods seem preferable.

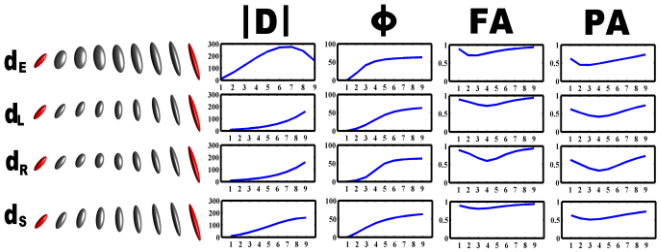

Fig. 3. Geodesic paths in experiment 5 between two general tensors (in red) and graphs of four measures.

D. Interpolation and Smoothing of Real Data

We smooth and interpolate (with 2 interpolations between each pair of original voxels) the diffusion tensor data from a normal human brain, and calculate the FA and PA maps shown in Figure 4. Obviously, FA and PA maps from the processed tensor data are much smoother than the ones without processing. The feature that the cingulum (cg) is distinct from the corpus callosum (cc) is clearer in the anisotropy maps from the processed data than those without processing in Fig. 4.

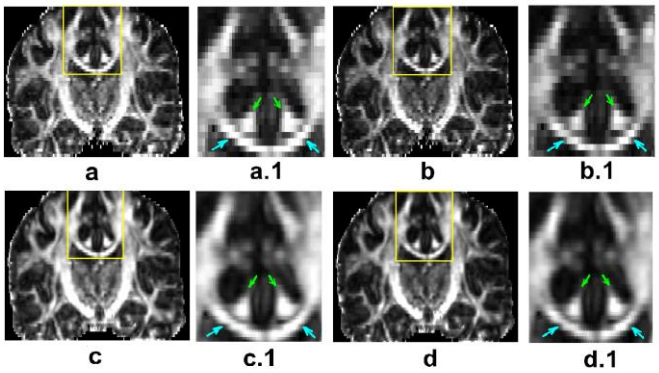

Fig. 4. FA (a) and PA (b) maps based on Bayesian estimates without post-processing. FA (c) and PA (d) maps from smoothed and interpolated tensor data obtained with the weighted generalized Procrustes method. (a.1), (b.1), (c.1) and (d.1) are zoomed inset region.

V. Conclusion

In this work, we have used the full ordinary Procrustes analysis to match two diffusion tensors. The solution to the full ordinary Procrustes problem of a diffusion tensor and an isotropy has been normalized to be a new anisotropy index-Procrustes Anisotropy (PA). PA provides better contrast in highly anisotropic region of the brain. For a more general

case with more than two tensors, the weighted generalized Procrustes framework has been developed for averaging more than two diffusion tensors with different fractions of contributions to the mean tensor. The weighted generalized Procrustes method has also been adapted for tensor field smoothing and interpolation. It will be interesting to apply Procrustes methods to other processing situations such as regularization of diffusion tensors [27] for the future work.

ACKNOWLEDGMENT

The work was supported by the European Commission FP6 Marie Curie program through the CMIAG Research Training Network. The diffusion MR image data used in this paper is provided by the Division of Academic Radiology, University of Nottingham and Queen's Medical Centre, UK.

REFERENCES

[1] D. C. Alexander, "Multiple-fibre reconstruction algorithms for diffusion MRI," *Annals of the New York Academy of Sciences*, vol. 1046, pp. 113–133, Jan. 2005.
[2] P. B. Kingsley, "Introduction to diffusion tensor imaging mathematics: Part iii. tensor calculation, noise, simulations, and optimisation," *Concepts in Magnetic Resonance Part A*, vol. 28, pp. 155–179, Mar. 2006.
[3] C. G. Koay, J. D. Carew, A. L. Alexander, P. J. Basser, and M. E. Meyerand, "Investigation of anomalous estimates of tensor-derived quantities in diffusion tensor imaging," *Magnetic Resonance in Medicine*, vol. 55 , pp. 930–936, Mar. 2006.
[4] T. Behrens, M. Woolrich, M. Jenkinson, H. Johansen-Berg, R. Nunes, S. Clare, P. Matthews, J. Brady, and S. Smith, "Characterisation and propagation of uncertainty in diffusion-weighted MR imaging," *Magnetic Resonance in Medicine*, vol. 50, pp. 1077–1088, Oct. 2003.
[5] D. Zhou, I. L. Dryden, A. Koloydenko, and L. Bai, "A Bayesian method with reparameterisationfor diffusion tensor imaging," in *Proc. of SPIE Medical Imaging 2008: Image Processing*, 2008, pp. 69142.
[6] D. L. Bihan, J. F. Mangin, C. Poupon, C. A. Clark, S. Pappata, M. Molko, and H. Chabriat, "Diffusion tensor imaging: concepts and applications," *Journal of Magnetic Resonance Imaging*, vol. 13, pp. 534–546, Mar. 2001.
[7] P. J. Basser, S. Pajevic, C. Pierpaoli, J. Duda, and A. Aldroubi, "In vivo fibre tractography using DT-MRI data," *Magnetic Resonance in Medicine*, vol. 44, pp. 625–632, Oct. 2000.
[8] S. Jbabdi, M. W. Woolrich, J. L.Andersson, and T. E. Behrens, "A Bayesian framework for global tractography," *Neuroimage*, vol. 37, pp. 116–29, April 2007.
[9] H. Sun, P. A. Yushkevich, H. Zhang, P. A. Cook, J. T. Duda, T. J. Simon, and J. C. Gee, "Shape-based normalization of the corpus callosum for (DTI) connectivity analysis," *IEEE Trans. on Medical Imaging*, vol. 26, pp. 1166–1178, Sept. 2007.
[10] V. Arsigny, P. Fillard, X. Pennec, and N. Ayache, "Log-Euclidean metrics for fast and simple calculus on diffusion tensors," *Magnetic Resonance in Medicine*, vol. 56, pp. 411–421, Jun. 2006.
[11] V. Arsigny, P. Fillard, X. Pennec, and N. Ayache, "Geometric means in a novel vector space structure on symmetric positive-definite matrices," *SIAM Journal on Matrix Analysis and Applications*, vol. 29, pp. 328–347, Feb. 2007.
[12] P. G. Batchelor, M. Moakher, D. Atkinson, F. Calamante, and A. Connelly, "A rigorous framework for diffusion tensor calculus," *Magnetic Resonance in Medicine*, vol. 53, pp. 221–225, Dec. 2004.
[13] A. Dryden, Koloydenko, and D. Zhou, "Non-Euclidean statistics for covariance matrices, with applications to diffusion tensor imaging," *Annals of Applied Statistics*, vol. 3, pp. 1102–1123, Mar. 2009.
[14] P. T. Fletcher and S. Joshi, "Riemannian geometry for the statistical analysis of diffusion tensor data," *Signal Process*, vol. 87, pp. 250–262, Jun. 2007.
[15] M. Fréchet, "Les éléments aléatoires de nature quelconque dans un espace distancié," *Annales de l'institut Henri Poincaré*, vol. 10, pp. 215– 310, Sept. 1948.
[16] R. Koenker, "The median is the message: toward the Fréchet median," *Journal de la Société Francqise de Statistique*, vol. 147, pp. 61–64, 2006.
[17] H. Le, "Mean Size-and-Shapes and Mean Shapes: A Geometric Point of View," *Advances in Applied Probability*, vol. 27, pp. 44–55, Aug. 1995.
[18] M. Moakher and P. G. Batchelor, "Symmetric Positive-Definite Matrices From Geometry to Applications and Visualization," *Visualization and Processing of Tensor Fields*, J. Weickert and H. Hagen, Ed. Springer, Germany, 2006, pp. 291–295.
[19] P. Fillard, X. Pennec, V. Arsigny, and N. Ayache, "Clinical DT-MRI estimation, smoothing, and fiber tracking with Log-Euclidean metrics," *IEEE Trans. on Medical Imaging*, vol. 26, pp. 1472–1482, Nov. 2007.
[20] X. Pennec, P. Fillard, and N Ayache, "A Riemannian framework for tensor computing," *International Journal of Computer Vision*, vol. 66, pp. 41–66, Jan. 2006.
[21] I. L. Dryden and K. Mardia, *Statistical Shape Analysis*, Wiley & Sons, Chichester, 1998.
[22] J. C. Gower, "Generalized Procrustes analysis," *Psychometrika*, vol. 40, pp. 33–50, Jan. 1975.
[23] D. G. Kendall, "A Survey of the Statistical Theory of Shape," *Statistical Science*, vol. 28, pp. 87–120, 1989.
[24] S. Sotiropoulos, L. Bai, P. Morgan, D. Auer, C. Constantinescu, and C. C. Tench, "A regularized two-tensor model fit to low angular resolution diffusion images using basis directions," *Journal of Magnetic Resonance Imaging*, vol. 28, pp. 199-209, Jun. 2008.
[25] P. J. Basser, J. Mattiello, and D. Le Bihan, "Estimation of the effective self-diffusion tensor from the NMR spin echo," *Journal of Magnetic Resonance, Series B*, vol. 103, pp. 247–254, 1994.
[26] C. E. C. Lee, L. E. Danielian, D. Thomasson, and E. H. Baker, "Normal regional fractional anisotropy and apparent diffusion coefficient of the brain measured on a 3T MR scanner," *Neuroradiology*, vol. 51, pp. 3–9, 2009.
[27] O. Coulon, D. C. Alexander, and S. R. Arridge, "Diffusion tensor magnetic resonance image regularisation," *Medical Image Analysis*, vol. 8, pp. 47–67, 2004.

Zhou Diwei is a lecturer in statistics, School of Technology, University of Wolverhampton from September 2009. She received her PhD degree in statistics from School of Mathematical Sciences, University of Nottingham, UK in 2010. She worked as a Marie Curie research fellow in University of Nottingham from September 2006 to September 2009. Her main research interest is statistical applications for medical image analysis. Dr. Zhou is a member of Royal Statistical Society (RSS), UK from 2006 to present. She is also a committee member of West Midlands group of RSS from September 2010.

Ian Dryden was awarded a PhD in statistics from the University of Leeds, UK in 1989 and a BSc (Hons) in mathematics with statistics from the University of Nottingham, UK in 1986. Ian is a Professor in the Department of Statistics at the University of South Carolina, Columbia, USA and held previous positions at the University of Nottingham, University of Leeds and University of Chicago. He has published over 100 articles including the monograph on Statistical Shape Analysis (Chichester, John Wiley and Sons, 1998) with K.V. Mardia. Ian's research interests include shape analysis; statistical image analysis; medical image analysis; spatial statistics; high-dimensional data analysis; and applications of statistics in bioinformatics, chemoinformatics, biomedical sciences, and computer science.

Professor Dryden is an elected Fellow of the Institute of Mathematical Statistics, an elected member of the International Statistical Institute, fellow of the Royal Statistical Society, and member of the American Statistical Association and International Biometric Society. He was recently the Chair of the Research Section of the Royal Statistical Society.

Alexey Alexandrovich Koloydenko was born in Voronezh, Russian Federation, on 8th June 1971. He received the B.S. degrees in physics and mathematics (with information systems minor) in 1994 from the Voronezh State University, Russian Federation and Norwich University, USA, respectively. He received in 1996 the M.S.(tech.) degree in physics and radio-electronics from the Voronezh State University, Russian Federation, and the M.S. degree in mathematics and statistics from the University of Massachusetts at Amherst, USA. He received the Ph.D. degree in mathematics and statistics from the University of Massachusetts at Amherst, USA, in 2000.

He held postdoctoral research and teaching positions with the Department of Mathematics and Statistics of the University of Massachusetts at Amherst, Statistics and Computer Science Departments of the University of Chicago, and Eurandom (research only), The Netherlands, in 2000, 2001--2002, and 2002--2005, respectively. In 2004--2005, while at Eurandom, he was on a secondment at Philips Medical Systems (Best, the Netherlands). He was a Lecturer in Statistics at the University of Nottingham, UK, in 2005-2008, and has been a lecturer
in Probability Theory and Statistics at Royal Holloway, University of London. His research interests include statistical processing and analysis of images, diffusion weighted MRI, statistical and machine learning, particularly hidden Markov models, and also algebraic aspects of probability theory and statistics. He has also contributed to the fields of natural image statistics and speech recognition.

Dr. Koloydenko was a member of the Pattern Analysis, Statistical Modelling and Computational Learning European network (PASCAL) in 2004--2008, and he has been a member of the British Machine Vision Association and Society for Pattern Recognition and a fellow of the Royal Statistical Society since 2009. He has also been a member of the Institute of Mathematical Statistics since 2010, when he also became a Fellow of the Higher Education Academy (HEA UK). In the past, he held student memberships of the American Mathematical Society (1994-2000) and Classification Society of North America (1998-2000).

Dr Li Bai has significant experience in pattern recognition, computer vision, and medical image analysis research. She has published 180+ articles in journals and conferences, and won a Most Cited Paper award for the journal of Image and Vision Computing. She has obtained, as Principal Investigator/Coordinator, multi-million pound research grants from UK and EU funding councils. Her research has also been funded by the UK industry, the US Army Laboratory, and the UK Technology Strategy Board. She is regular referee for numerous journals and has been a member of the EPSRC Peer Review College for more than 10 years..